

Numerical modeling of quantum beam generation from ultra-intense laser-matter interactions

TATSUFUMI NAKAMURA¹ AND TAKEHITO HAYAKAWA²

¹Fukuoka Institute of Technology, Fukuoka, Japan

²Japan Atomic Energy Agency, Tokai, Japan

(RECEIVED 14 December 2014; ACCEPTED 9 February 2015)

Abstract

When intense laser beams interact with solid targets, high-energy photons are effectively generated via radiation reaction effect. These photons receive a large portion of the incident laser energy, and the energy transport by photons through the target is crucial for the understanding of the laser–matter interactions. In order to understand the energy transport, we newly developed a Particle-in-Cell code which includes the photon–matter interactions by introducing photon macro-particles. Test simulations are performed and compared with simulations using a particle transport code, which shows a good agreement.

Keywords: Gamma-ray transport; Intense laser; Particle-in-Cell simulation; Quantum beam generation

1. INTRODUCTION

Interactions of intense laser beams and matters have attracted much attention from various aspects including fast ignition in inertial fusion (Tabak *et al.*, 1994), laboratory astrophysics (Remington *et al.*, 1999), and generations of high-energy particles (Tajima & Dawson, 1979; Murnane *et al.*, 1991; Hatchett *et al.*, 2000). In the regime where the radiation reaction effects on an electron motion in a laser field, the electron motion becomes dissipative, which results in decreasing of the electrons maximum energy (Zhidkov *et al.*, 2002) and ions energy (Naumova *et al.*, 2009; Tamburini *et al.*, 2010). By paying attention to the fact that the electron energy dissipates in the form of the radiation, it is proposed that when the laser and plasma parameters are properly chosen high-energy photons can be effectively generated by the irradiation of ultra-intense laser on solid target (Nakamura *et al.*, 2012; Ridgers *et al.*, 2012), which shows the possibility of a unique source of gamma-rays with its high intensity.

For the further understanding of the interactions of ultra-intense laser beams and matters, exploring of the energy transport inside of the target is needed, that is, the understanding of the energy transport by high flux of gamma-ray is crucial. In order to investigate numerically the gamma-ray

transport in targets, relevant photon–matter interaction processes should be treated as well as the collective motion of plasmas. Particle-in-Cell (PIC) codes are widely used for investigating the intense laser–matter interactions. The PIC codes deal with the time evolution of electromagnetic field and charged particles motion self-consistently but without the above mentioned photon–matter interactions yet.

In this paper, we explain the modeling of the photon–matter interactions in the PIC code. In Section 2, the introduction of macro-particle of gamma-ray in the PIC code is explained, and the treatment of relevant photon–matter interactions are described. In Section 3, the test calculations of gamma-ray transport inside of a carbon target is performed and the result is compared with the results by using Particle and Heavy Ion Transport code System (PHITS). Conclusions are given in Section 4.

2. NUMERICAL MODELING ON GAMMA-RAY TRANSPORT IN PIC CODE

In PIC simulations, an electromagnetic field is treated as a wave. Its temporal evolution is calculated by solving Maxwell equations. When solving Maxwell equations, spatial grids are introduced and the electromagnetic fields are defined on the grid points. The introduction of the grids limits the shortest wavelength resolved in the simulation (Birdsall & Langdon, 1985). Therefore, it is not reasonable to treat the propagation of photons in the gamma-ray

Address correspondence and reprint requests to: Tatsufumi Nakamura, Fukuoka Institute of Technology, Fukuoka 811-0295, Japan. E-mail: t-nakamura@fit.ac.jp

regime using Maxwell equations, since it requires an unreasonable numbers of grid points. Thus, in our code, the gamma-rays are treated as photon macro-particles in the same way as charged particles.

2.1. Generation of Gamma-rays in PIC Code

In the interactions of ultra-intense laser beams and matters, the electron motion becomes dissipative due to the radiation reaction effect. In this paper, we pay our attention on the regime where the quantum effect in the radiation reaction is weak, that is, $\chi_e = e\hbar\sqrt{(F_{\mu\nu}p^\nu)^2}/mcE_S \sim \gamma_e E/E_S \ll 1$, where the emitted photon energy is relatively smaller than the electron energy and the energy dissipation process is treated as a continuous damping process. Here, m, e, c , and \hbar are the electron rest mass, the electric charge, the speed of light, and the Planck's constant, respectively. $F_{\mu\nu}, p_\mu$ are the field tensor and four-momentum, and E is the laser electric field and $E_S \sim 1.3 \times 10^{18}$ V/m is the Schwinger field. The damping of the momentum in this regime is evaluated by using Landau–Lifshitz equation, which is incorporated in PIC code with reasonable computational load (Tamburini *et al.*, 2010). It is numerically shown that high-energy photons are effectively generated via radiation reaction effect, where the conversion efficiency reaches 20–30% when the optimum parameters are chosen (Nakamura *et al.*, 2012; Ridgers *et al.*, 2012). The energy spectrum of radiation is evaluated by post-processing with the classical form of synchrotron radiation formula for a single electron;

$$\frac{dI}{d\omega} \cong 2\sqrt{3}\frac{e^2}{c}\gamma\frac{\omega}{\omega_c}\int_{2\omega/\omega_c}^{\infty} K_{5/3}(x)dx, \quad (1)$$

where $\omega_c = 3\gamma^3 c/\rho$ and $K_{5/3}(x)$ is the modified Bessel function. Here, γ and ρ are the electron Lorentz factor and the curvature radius of the electron trajectory, respectively. By summing up the contribution from the electrons which are decelerated by radiation reaction, we can obtain the energy spectrum of radiated photons via radiation reaction. In Figure 1, the radiation spectrum via radiation reaction calculated by the PIC code PREIM (Nakamura *et al.*, 2010) is plotted as a red dotted line, where the laser pulse having the normalized amplitude of $a = 150$, a power of 10 PW, and duration of 30 fs irradiates on a solid carbon target attached with preplasma having scale length of $L = 2.5$ μm .

Here we consider the energy transport by photons. We introduce macro-particles of photons in order to reproduce the above spectrum by the ensemble of the introduced photons. The photon emission of the energy below $E \leq 10$ keV is not included, since we are interested in the physics related to the photons in the gamma-ray regime. But even in this case, the electrons motion is calculated by Landau–Lifshitz equation and energy loss via radiation reaction is taken into account. In each time step of calculations, the frequency ω_c is calculated from the trajectory of accelerated electrons.

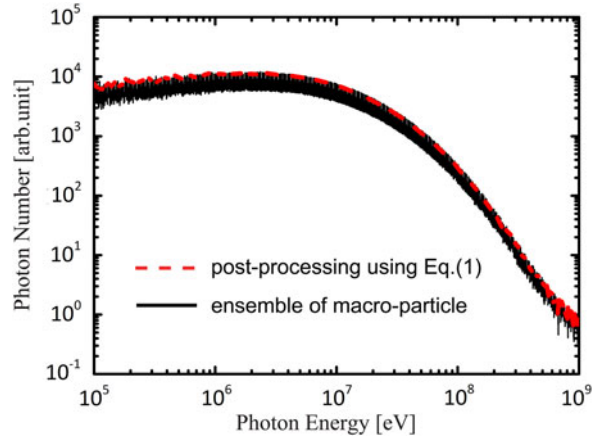


Fig. 1. Comparison of energy spectrum evaluated by synchrotron radiation formula as post-processing (dotted line), and ensemble of the macro-particle of gamma-rays introduced in PIC (solid line).

Then the emitted photon energy is determined by randomly sampling from the synchrotron radiation profile where the probability is proportional to the spectrum intensity. Next, the weight of the macro-particle is determined from the energy conservation, that is, the weight of the electron macro-particle times the electron energy loss equals to the weight of the photon macro-particle times the determined photon energy. In this manner, photons are generated in each time step of calculations when the electrons lose their energies by radiation reaction. The energy spectrum calculated from the photon macro-particle is plotted in Figure 1 as the black line. The spectrum of the photon macro-particle well reproduces the spectrum evaluated by Eq. (1).

The direction of photon momentum is also determined from the formula for the radiation emission direction from a single electron (Landau & Lifshitz, 1975);

$$\frac{dI}{d\Omega} = \frac{e^2}{4\pi c^3} \left\{ \frac{2(\mathbf{n} \cdot \mathbf{w})(\mathbf{v} \cdot \mathbf{w})}{[c[1 - (\mathbf{v} \cdot \mathbf{n})c]^5} + \frac{\mathbf{w}^2}{[1 - (\mathbf{v} \cdot \mathbf{n})c]^4} - \frac{(1 - v^2/c^2)(\mathbf{n} \cdot \mathbf{w})^2}{[1 - (\mathbf{v} \cdot \mathbf{n})c]^6} \right\}, \quad (2)$$

where \mathbf{n} is the unit vector in the emission direction, \mathbf{v} and $\mathbf{w} = \dot{\mathbf{v}}$ are the electron velocity and acceleration, respectively. After determining the photon energy, momentum, and weight, the photon macro-particle is generated at the position of the corresponding electron, and it propagates in the simulation box with the speed of light. Figure 2 shows the temporal evolution of the photon distributions, where the simulation condition is chosen as same as that in Figure 1.

2.2. Transport of Gamma-rays in PIC Code

The photons propagate through the target interacting with atoms and atomic nucleus. This photon propagation results in the absorption and scattering of photons and in the generation of charged particles and nucleons. In Figure 3, the photo-cross-section for a carbon atom is plotted. For photons

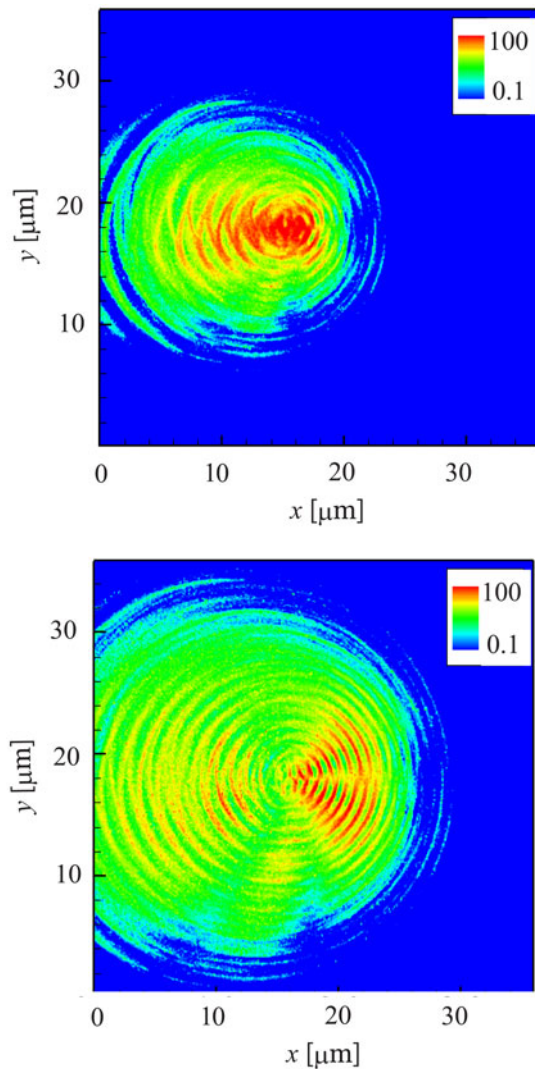


Fig. 2. Photon number densities of different timing is plotted, where the density is normalized by the critical density. The lower figure corresponds to 20 fs later from the upper figure.

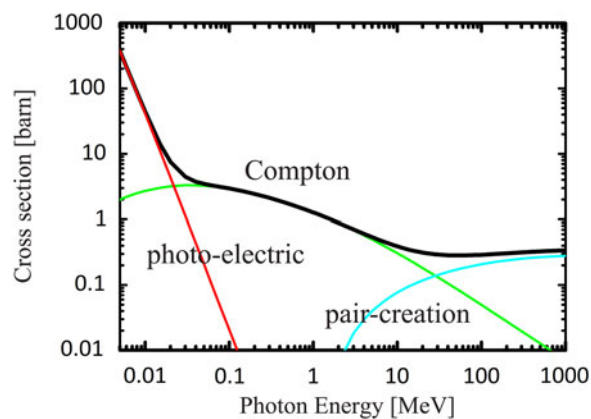


Fig. 3. Photo-cross-section for a carbon atom.

with the energy higher than tens of keV the cross-section is dominated by that of Compton scattering, where a photon collides with a bound electron and some portion of energy is transferred to the electron becoming a free electron. For photons with energies beyond tens of MeV, the cross-section is dominated by that of pair-creation where the photon energy is materialized under the electric field of nucleus resulting on the creation of an electron–positron pair.

First, we consider the modeling of Compton scattering process in a PIC code. The total cross-section of Compton scattering is expressed by integrating the Klein–Nishina formula (Klein & Nishina, 1929; Weinberg, 1995) over the solid angle;

$$\sigma = \frac{3}{4} \sigma^{\text{Th}} \left\{ \frac{1+\epsilon}{\epsilon^3} \left[\frac{2\epsilon(1+\epsilon)}{1+2\epsilon} - \log(1+2\epsilon) \right] + \frac{\log(1+2\epsilon)}{2\epsilon} - \frac{1+3\epsilon}{(1+2\epsilon)^2} \right\}, \quad (3)$$

where $\sigma^{\text{Th}} = 8\pi r_e^2/3 \sim 0.67$ [barn] is the cross-section of Thomson scattering and $\epsilon = \hbar\omega/mc^2$. Here, r_e is the electron classical radius and mc^2 expresses the electron rest energy. Using the total cross-section, the probability of Compton scattering to take place during a time step Δt is obtained as $\nu = n_{\text{atom}}\sigma(c\Delta t)$, where n_{atom} is the number density of carbon atoms. Using the scattering probability, the occurrence of Compton scattering is determined by the Monte Carlo manner.

When Compton scattering is determined to take place, the photon scattering angle is determined using the differential cross-section;

$$\frac{d\sigma}{d\Omega} = \frac{r_e^2}{2} \frac{1 + \cos^2\theta}{2[1 + \epsilon(1 - \cos\theta)]} \left\{ 1 + \frac{\epsilon^2(1 + \cos\theta)^2}{[1 + \epsilon(1 - \cos\theta)](1 + \cos^2\theta)} \right\}, \quad (4)$$

which is plotted in Figure 4, where θ is the photon scattering angle.

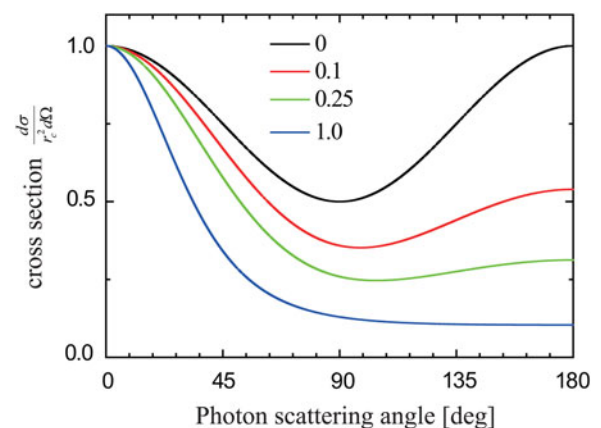


Fig. 4. Differential cross-section of Compton scattering as a function of photon scattering angle. Lines with different colors correspond to the different values of ϵ .

When the photon scattering angle is determined, the scattered photon energy, the scattered electron energy and angle are also calculated as

$$E^{\text{ph}} = \frac{\hbar\omega}{1 + \varepsilon(1 - \cos\theta)}, \quad (5)$$

$$E^{\text{ele}} = \frac{\hbar\omega(1 - \cos\theta)}{1 + \varepsilon(1 - \cos\theta)}. \quad (6)$$

Then the photon energy is modified. A new-born electron is generated at the position of the incident photon.

The pair-creation is treated in the same way as Compton scattering, that is, to determine first the event occurrence by using the cross-section which is given by Bethe and Heitler (1934), then the angle and energy by Monte Carlo manner. The difference from Compton scattering is that the photon is annihilated and a pair of electron and positron is created. The high-energy photons also interact with the nuclei through Giant Dipole Resonance, where a relatively large cross-section exists around MeV region known. The atomic nucleus is excited by the absorption of an incident photon. The excited nucleus de-excites to the ground state by emitting gamma-ray or to another nucleus by emitting a nucleon (proton, neutron, α -particle, etc.). In our code, photo-nuclear reaction of (γ, n) process is also included by Monte Carlo methods as in the same manner as Compton scattering and pair-creation.

3. TEST SIMULATION: COMPARISON WITH RADIATION TRANSPORT CODE

Calculations of photon transports in carbon targets are performed using the newly developed PIC code in order to compare with the radiation transport code called PHITS which is developed in JAEA (Sato *et al.*, 2013). The simulation conditions in the PHITS calculation is that a single photon with energy of 5 MeV irradiates the carbon target having the mass density of 2 g/cc with a cubic geometry of 1 mm³. 10⁷ events in total are calculated. In three-dimensional PIC calculation, the same number of photons irradiate the target with the same configuration. In order to adopt the test particle approximation, we do not solve Maxwell equations and plasma motion is not included. The results are compared in Figure 5, where the energy spectra of photons, electrons, and positrons are plotted for PHITS calculation and PIC calculation, respectively. Here, the numbers of the particles are normalized by the incident photon number.

Photons are scattered by Compton scattering, resulting in the generation of low-energy photons with rather uniform distribution ranging from $E_{\text{min}} = \hbar\omega/(1 + 2\hbar\omega/mc) \sim 0.24$ –5 MeV. Electrons are generated by Compton scattering, and also by pair-creation together with positrons. Total number of electrons per source are 2.51×10^{-3} , and that of positron is 1.87×10^{-4} in PHITS calculation. These numbers are in

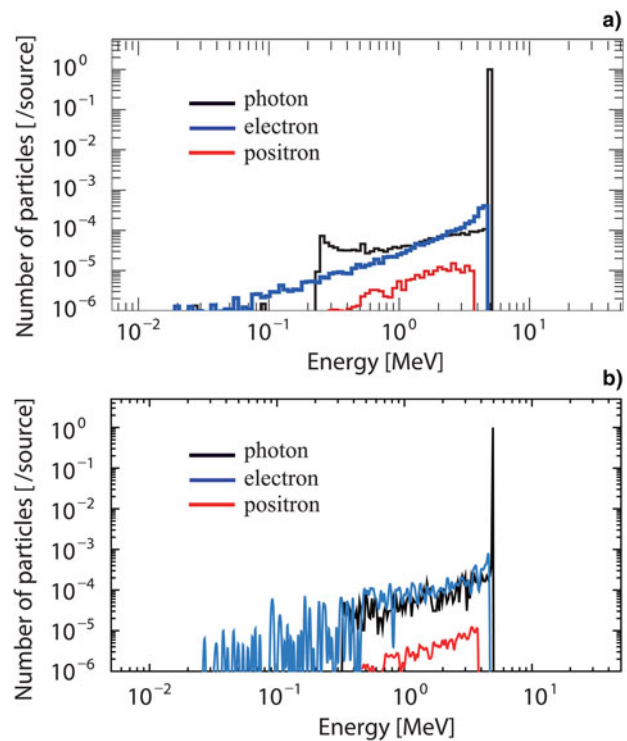


Fig. 5. Energy spectra of photons, electrons, and positrons generated by 5 MeV photon irradiation on carbon target, calculated by (a) PHITS and (b) PIC codes.

good agreement with the PIC results which are 2.64×10^{-3} for electrons and 1.01×10^{-4} for positrons, respectively.

4. CONCLUSIONS

We have modeled the high-energy photon transport in a matter to include it in a PIC code which could be used to investigate the energy transport in ultra-intense-laser-matter interactions. In order to simplify the modeling, the attention is paid on the photon-matter interaction in the regime $E > 10$ keV, where Compton scattering and pair-creation is the dominant processes in the photon-atom interaction. This could be justified for the laser-matter interaction in the radiation reaction dominated regime, since a large portion of laser energy is converted into gamma-rays, and the energy transport by photons is dominated by the laser-driven gamma-rays. The developed code is tested using the PHITS code, and shows a good agreement on energy spectra of generated particles.

Our code is applicable for a thin or low-Z target where photon generation via Bremsstrahlung is negligibly small. Since the energy coupling from laser to gamma-rays via radiation reaction reaches 20–30%, their energy transport dominates over the energy transport by the Bremsstrahlung photons unless the large portions of laser-accelerated electrons energy is converted into the Bremsstrahlung photons.

In the future work, the interaction of ultra-intense laser beams and matters will be investigated by our code to explore the energy transport inside of the targets.

ACKNOWLEDGMENTS

Authors thank Drs S. Bulanov, T. Esikepov, M. Kando, and J. Koga for discussions. This work is partially supported by KAKENHI (grant no. 25400540). This research used computational resources of the K computer and other computers of the HPCI system provided by the AICS and through the HPIC System Research Project (Project ID: hp120037, hp140122).

REFERENCES

- BETHE, H. & HEITLER, W. (1934). On the stopping of fast particles and on the creation of positive electrons. *Proc. R. Soc. A* **146**, 83–112.
- BIRDSALL, C. & LANGDON, A.B. (1985). *Plasma Physics via Computer Simulation*. New York: McGraw-Hill.
- HATCHETT, S.P., BROWN, C.G., COWAN, T.E., HENRY, E.A., JOHNSON, J.S., KEY, M.H., KOCH, J.A., LANGDON, A.B., LASINSKI, B.F., LEE, R.W., MACKINNON, A.J., PENNINGTON, D.M., PERRY, M.D., PHILLIPS, T.W., ROTH, M., SANGSTER, T.C., SINGH, M.S., SNAVELY, R.A., STOYER, M.A., WILKS, S.C. & YASUIKE, K. (2000). Electron, photon, and ion beams from the relativistic interaction of petawatt laser pulse with solid targets. *Phys. Plasmas* **7**, 2076–2082.
- KLEIN, O. & NISHINA, Y. (1929). Über die streuung von strahlung durch freie elektronen nach der neuen relativistischen quantendynamik von Dirac. *Z. Phys.* **52**, 853–868.
- LANDAU, L.D. & LIFSHITZ, E.M. (1975). *The Classical Theory of Fields*. Oxford: Pergamon.
- MURNANE, M.M., KAPTEYN, H.C., ROSEN, M.D. & FALCONE, R.W. (1991). Ultrafast x-ray pulses from laser-produced plasmas. *Science* **251**, 531–536.
- NAKAMURA, T., KOGA, J.K., ESIKEPOV, T.Z., KANDO, M., KORN, G. & BULANOV, S.V. (2012). High-power gamma-ray flash generation in ultraintense laser-plasma interactions. *Phys. Rev. Lett.* **108**, 195001.
- NAKAMURA, T., TAMPO, M., KODAMA, R., BULANOV, S.V. & KANDO, M. (2010). Interaction of high contrast laser pulse with foam-attached target. *Phys. Plasmas* **17**, 113107.
- NAUMOVA, N., SCHLEGEL, T., TIKHONCHUK, V.T., LABAUNE, C., SOKOLOV, I.V. & MOUROU, G. (2009). Hole boring in a DT pellet and fast-ion ignition with ultraintense laser pulses. *Phys. Rev. Lett.* **102**, 025002.
- REMINGTON, B.A., ARNETT, D., DRAKE, R.P. & TAKABE, H. (1999). Modeling astrophysical phenomena in the laboratory with intense lasers. *Science* **284**, 1488–1493.
- RIDGERS, C.P., BRADY, C.S., DUCLOUS, R., KIRK, J.G., BENNETT, K., ARBER, T.D., ROBINSON, A.P.L. & BELL, A.R. (2012). Dense electron-positron plasmas and ultraintense gamma rays from laser-irradiated solids. *Phys. Rev. Lett.* **108**, 165006.
- SATO, T., NIITA, K., MATSUDA, N., HASHIMOTO, S., IWAMOTO, Y., NODA, S., OGAWA, T., IWASE, H., NAKASHIMA, H., FUKUHORI, T., OKUMURA, K., KAI, T., CHIBA, S., FURUTA, T. & SIHVER, L. (2013). Particle and heavy ion transport code system PHITS, version 2.52. *J. Nucl. Sci. Technol.* **50**, 913–923.
- TABAK, M., HAMMER, J., GLINSKY, M., KRUEER, W.L., WILKS, S.C., WOODWORTH, J., CAMPBELL, E.M., PERRY, M.D. & MASON, R.J. (1994). Ignition and high gain with ultrapowerful lasers. *Phys. Plasmas* **1**, 1626–1634.
- TAJIMA, T. & DAWSON, J.M. (1979). Laser electron accelerator. *Phys. Rev. Lett.* **43**, 267–270.
- TAMBURINI, M., PEGORARO, F., PIAZZA, A.D., KEITEL, C.H. & MACCHI, A. (2010). Radiation reaction effects on radiation pressure acceleration. *New J. Phys.* **12**, 123005.
- WEINBERG, S. (1995). *The Quantum Theory of Fields 1*. Cambridge: Cambridge University Press.
- ZHIDKOV, A., KOGA, J., SASAKI, A. & UESAKA, M. (2002). Radiation damping effects on the interaction of ultraintense laser pulses with an overdense plasma. *Phys. Rev. Lett.* **88**, 185002.